

Dear author,

Please note that changes made in the online proofing system will be added to the article before publication but are not reflected in this PDF.

We also ask that this file not be used for submitting corrections.



ELSEVIER

Available online at [www.sciencedirect.com](http://www.sciencedirect.com)

ScienceDirect

Current Opinion in  
Chemical Biology

# Visualizing glycans on single cells and tissues

Ben Ovryn, Jie Li, Senlian Hong and Peng Wu

## Address

Department of Chemical Physiology, The Scripps Research Institute,  
10550 N Torrey Pines Rd, La Jolla, CA 92037, United States

Corresponding authors: Ovryn, Ben ([benovryn@scripps.edu](mailto:benovryn@scripps.edu)) and Wu,  
Peng ([pengwu@scripps.edu](mailto:pengwu@scripps.edu))

Current Opinion in Chemical Biology 2017, 39:xx–yy

This review comes from a themed issue on **Molecular imaging**

Edited by **Xing Chen** and **Yanyi Huang**

<http://dx.doi.org/10.1016/j.cbpa.2017.04.018>

1367-5931/© 2017 Published by Elsevier Ltd.

## Imaging without genetically expressed probes

Glycans coating the surface of archaea, bacteria and eukaryotes have attracted significant attention of chemists and biologists in this Post-Genome Era. These biomacromolecules are not directly encoded in the genome, and the non-template driven, posttranslational modification presents grand challenges to the study of their molecular functions in native environments [1]. Development of bioorthogonal chemistry has provided a paradigm shifting solution enabling novel approaches to unravel the dynamic complexity of glycosylation. The term bioorthogonal was introduced into the published literature in 2003 by C.R. Bertozzi [2], to refer to reactions that neither interact nor interfere with the cell's biochemistry [3–5]. Installing a probe on glycans with a two-step bioorthogonal chemical reporter strategy requires the introduction of a reporter into cellular glycans and a chemical reaction that forms a stable covalent linkage between the reporter and the probe molecule. In addition to the requirement that the reaction is essentially not toxic, the reaction rate needs to be fast enough (in the biological milieu) in order to capture the kinetics of the cellular processes of interest. Several reactions have proven to be bioorthogonal [6]. Two of the earliest reactions introduced by the Bertozzi group are the Staudinger ligation [3] and 'copper-free click chemistry' which is a 1,3-dipolar cycloaddition between azides and cyclooctynes (strain-promoted azide-alkyne cycloaddition (SPAAC)) [7,8<sup>\*</sup>]. More recently, it has been shown that the ligand-accelerated CuAAC (Cu(I)-catalyzed azide alkyne cycloaddition) can be exploited as a bioorthogonal reaction [6,9,10,11<sup>\*\*</sup>].

Two broad approaches incorporate the principles of a bioorthogonal chemical reporter strategy. The metabolic

oligosaccharide engineering approach, exploits the metabolic replacement of a monosaccharide by modified sugar analogues [12], while the chemoenzymatic glycan labeling (CeGL) exploits a recombinant glycosyltransferase to transfer a mono-saccharide analogue from a nucleotide sugar donor to a specific glycan acceptor [13<sup>\*</sup>]. In this short review, we highlight several recent innovative applications of these two approaches to imaging glycans on single cells and tissues, rather than presenting a chronological list of the many outstanding imaging advances (e.g. [8<sup>\*</sup>,14,15]). Although the focus here is the application of these approaches to imaging surface glycans, the recent tagging of intracellular carbohydrates in living cells [16] and the use of a bioorthogonal reporter strategy for Raman imaging [17<sup>\*</sup>], suggests that these approaches have a bright future. The recently reported MRI imaging of glycosylated tissue in live mice using metabolic labeling and a bioorthogonal gadolinium based probe [18], suggests that we can anticipate correlated optical and MRI imaging of glycans in live animals.

Unlike super-resolution imaging with genetically expressed probes, imaging the dynamics of biological processes with bioorthogonal chemical reporter strategies is fundamentally limited by the second-order rate constants associated with the bioorthogonal reaction [6,19–21]. The Staudinger ligation (with rate constants in the range of  $10^{-4}$  to  $10^{-2}$   $M^{-1} s^{-1}$ ) and SPAAC (with rate constants in the range of  $10^{-2}$  to  $1$   $M^{-1} s^{-1}$ ) are an order of magnitude slower than CuAAC reactions (with rate constants greater than  $10^1$  to  $10^2$   $M^{-1} s^{-1}$ ). Fortunately, older reactions continue to learn new tricks. For example, Wu's group has demonstrated that the introduction of an electron-donating picolyl azide combined with tris(triazolylmethyl)-amine-based ligand for Cu(I) (BTTPS) produced at least a 20-fold enhancement of CuAAC fluorescent labeling (with 1 nM concentration of metabolic precursor); this accelerated reaction enabled confirmation that the conversion rate of a monosaccharide building block into a cell-surface glycoconjugate is of order minutes [22<sup>\*\*</sup>].

## Imaging an ensemble of glycans in live cells

Studies using fluorescent recovery after photobleaching (FRAP) imaging of an ensemble of antibody labeled glycoproteins in the 1980s and early 1990s demonstrated that the extent of glycosylation and the size of the extracellular domain limit translational diffusion [23,24]. Attempts to understand and model how barriers in the cytoplasm, membrane bilayer and the external space separately restrict the translational (lateral) mobility of transmembrane proteins, showed that the diffusion of transmembrane glycoproteins was constrained as compared with the relatively free movement of glycosylphosphatidylinositols (GPI) proteins (typically

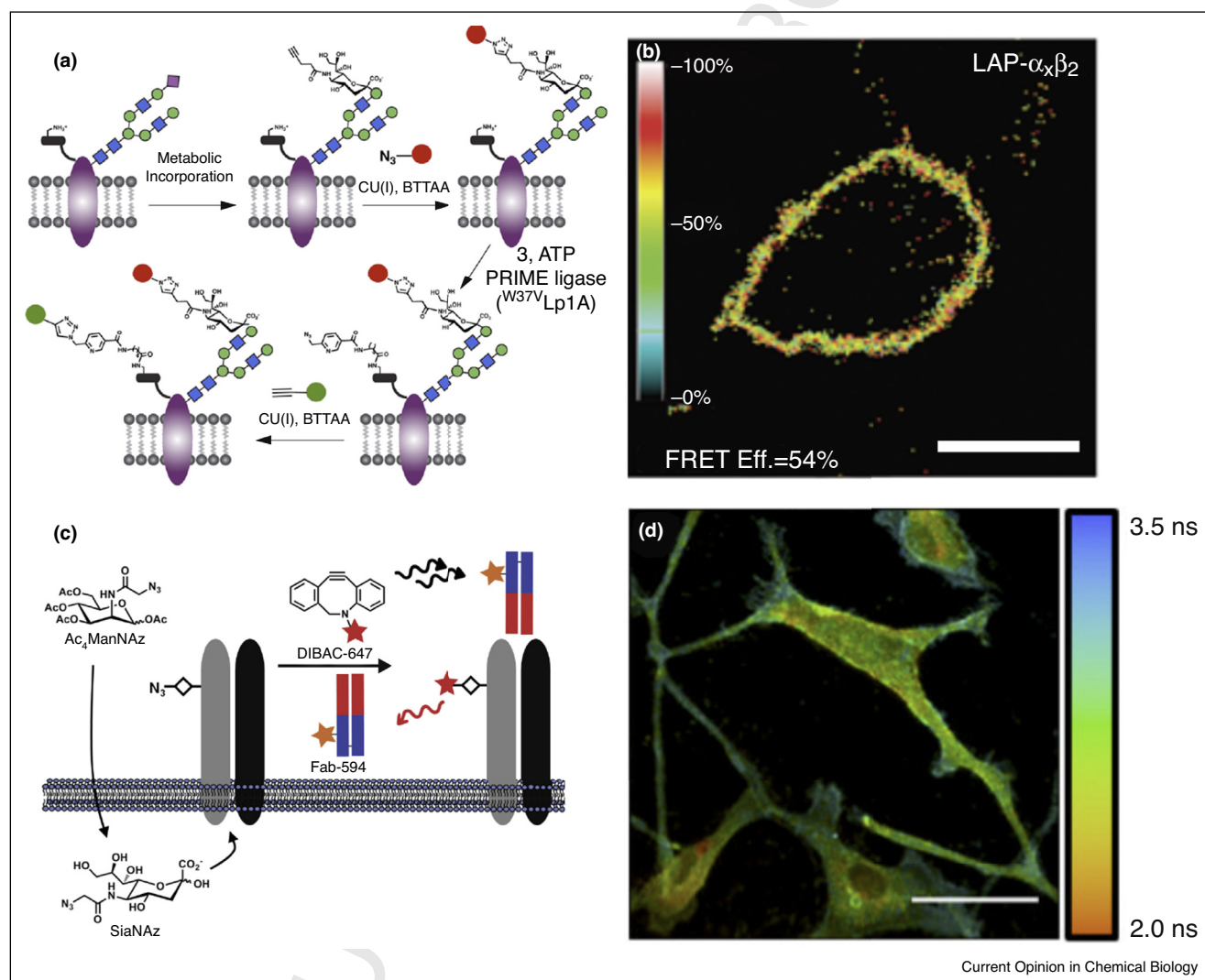
## 2 Molecular imaging

glycolipids diffuse 3 times the distance of transmembrane proteins before experiencing a barrier) [25]. FRAP measurements by Edidin's group using class I MHC molecules revealed that mutants with reduced N-linked glycans have increased lateral diffusion as compared with wild-type and that a large mobile fraction of diffusing glycoproteins enabled bleached regions to become repopulated with fluorescent molecules [24]. In contrast to these pioneering studies, contemporary FRAP imaging of the dynamics of glycolipids within the cell envelope of mycobacterial membranes

exploits the power of metabolically incorporated analogues [26].

Ensemble measurements of metabolically labeled glycans, co-labeled with a site specific protein tag, enabled Lin *et al.* to apply Förster resonance energy transfer (FRET) imaging to specific glycoproteins in live cells [27]. Using the enzyme-catalyzed probe ligation method, based upon lipoic acid ligase (LpIA), developed by Ting's group [28], a FRET donor was installed on an extracellular terminus of a protein of interest. As shown in Figure 1a,

Figure 1



Förster resonance energy transfer microscopy (FRET) of glycoproteins in live cells. **(a)** Bioorthogonal labeling in cells expressing a protein fused with LAP at the N-termini and incubated with  $Ac_4ManNAz$ . The FRET acceptor dye molecule (Alexa Fluor 647) using CuAAC assisted by BTAA. Subsequently, LAP was conjugated with the lipoic acid-picolyl azide derivative using  $W37V$ LpIA and followed by reaction with the FRET donor (Alexa Fluor 488-alkyne). Adapted from Lin *et al.* [27]. **(b)** FRET efficiency calculated using acceptor photobleaching in live HEK 293T cells expressing LAP- $\alpha_x\beta_2$  integrins. Scale bar = 10  $\mu$ m. Adapted from Lin *et al.* [27]. **(c)** Fab fragment targeting moiety used to place the donor fluorophore (Fab-594) as combined with metabolic labeling with  $Ac_4ManNAz$  to introduce the acceptor cyclooctyne-fluorophore (DIBAC-647) via a bioorthogonal reaction. Adapted from Belardi *et al.* [29]. **(d)** Two-photon microscopy employing time correlated single photon counting to measure FRET with fluorescence lifetimes using a Fab fragment to install a fluorescent donor (Alexa Fluor 594) on the glycoprotein backbone and metabolic labeling with  $Ac_4ManNAz$  to place an acceptor on integrins. Scale bar = 50  $\mu$ m. Adapted from Belardi *et al.* [29].

130 following metabolic incorporation with an alkyne reporter  
131 (e.g. Ac<sub>4</sub>ManNAI labeled sialic acid) into cell-surface  
132 sialylated glycans, an Alexa fluor-azide was installed as  
133 a FRET acceptor using CuAAC assisted by BTAA.  
134 Subsequently, LplA Acceptor Peptide (LAP) was conju-  
135 gated with a liponic acid-picolyl azide derivative followed  
136 by reaction with Alexa fluor-alkyne as the FRET donor.  
137 **Figure 1b** shows the FRET efficiency calculated using  
138 acceptor photobleaching in live HEK 293T cells expres-  
139 sing LAP- $\alpha_X\beta_2$  integrins. Because this method yielded  
140 relatively high levels of FRET ( $\approx 50\%$ ), Lin *et al.* were  
141 able to apply the approach to elucidate the role of sialyla-  
142 tion in the activation of  $\alpha_X\beta_2$  integrins [27]. Following  
143 confirmation using FRET imaging that the fluorinated  
144 sialic acid analogue 3F<sub>ax</sub>-Neu5Ac effectively inhibited the  
145 sialylation of  $\alpha_X\beta_2$  integrins, they showed that the removal  
146 of sialic acids impaired  $\alpha_X\beta_2$  integrin activation. They also  
147 demonstrated FRET imaging of glycosylated receptors  
148 such as sialylated glycans of epidermal growth factor  
149 receptor (EGFR).

150  
151 An alternative approach to implementing intensity based  
152 FRET measurements on a specific glycoprotein, Belardi  
153 *et al.* employed time correlated single photon counting  
154 with two-photon microscopy to measure fluorescence  
155 lifetimes [29]. After confirming that  $\alpha_V\beta_3$  integrin in  
156 U87MG cells is sialylated with  $\alpha 2,3$ -linked residues, they  
157 used a Fab fragment to install a fluorescent donor (Alexa  
158 Fluor 594) on the glycoprotein backbone and metabolic  
159 labeling with Ac<sub>4</sub>ManNAz to place an acceptor on integ-  
160 rin SiaNAz residues (**Figure 1c**). The measured lifetimes  
161 from FRET on  $\alpha_V\beta_3$  integrins in U87MG cells cultured  
162 with Ac<sub>4</sub>ManNAz is shown in **Figure 1d**. Histograms of  
163 the fluorescence lifetimes indicate that FRET reduced  
164 the lifetime of FAB-594 from 3.09 ns, *in vitro*, to an  
165 average of 2.60 ns in Ac<sub>4</sub>ManNAz tagged cells. They also  
166 confirmed that sialidase cleavage of SiaNAz residues  
167 essentially eliminated FRET.  
168

### 169 Single molecule tracking and super-resolution

170 With the explosion of single molecule tracking and super-  
171 resolution imaging of proteins (genetically encoded with  
172 photo-activatable fluorescent proteins or labeled with  
173 quantum dots or dye molecules), the extension of these  
174 approaches to glycoproteins was inevitable. Super-reso-  
175 lution imaging of glycans was demonstrated by two  
176 groups who published within a several month span in  
177 2014 using stochastic optical reconstruction microscopy  
178 (STORM) on live [30,31\*\*] and fixed cells [32\*\*]. One of  
179 these two groups also implemented single particle track-  
180 ing to follow glycans metabolically labeled with dye  
181 molecules (using biocompatible BTTPS/Cu<sup>I</sup> catalyst)  
182 [30,31\*\*]. Tracking of O-linked and N-linked sialylated  
183 proteins metabolically labeled with Ac<sub>4</sub>GalNAz and  
184 Ac<sub>4</sub>ManNAI, respectively, and tagged with dyes on can-  
185 cer cells revealed constrained diffusion which was mod-  
186 eled as damped Brownian motion resulting from a

186 confining harmonic potential [31\*\*]. The slower diffusion  
187 of glycans on cells with higher metastatic potentials was  
188 conjectured to be caused by increased crowding of surface  
189 glycoproteins which could effect the formation of adhe-  
190 sions to the extracellular matrix [33].  
191

192 An example of a ‘snapshot’ of the distribution of diffusing  
193 Alexa Fluor 647 dye molecules tagged to N-linked sialic  
194 acids on the surface of a live cancer cell is shown in  
195 **Figure 2a** (scale bar = 20  $\mu\text{m}$ ). **Figure 2b** shows a STORM  
196 image of N-linked sialic acid in HeLa cells metabolically  
197 labeled with Ac<sub>4</sub>ManNAI and conjugated with Alexa  
198 Fluor 647 azide (scale bar = 10  $\mu\text{m}$ ) [31\*\*]. **Figure 2c**  
199 and **d** show STORM images of a fixed human osteosar-  
200 coma (U2OS) cell metabolically labeled with Ac<sub>4</sub>GalNAz  
201 and clicked with (c) CuAAC and (d) SPAAC [34] (boxed  
202 region = 2.0  $\mu\text{m}$  wide). These super-resolution images  
203 highlight membrane nanotubes and adhesive filaments.  
204

### 205 Tissue and whole-animal imaging

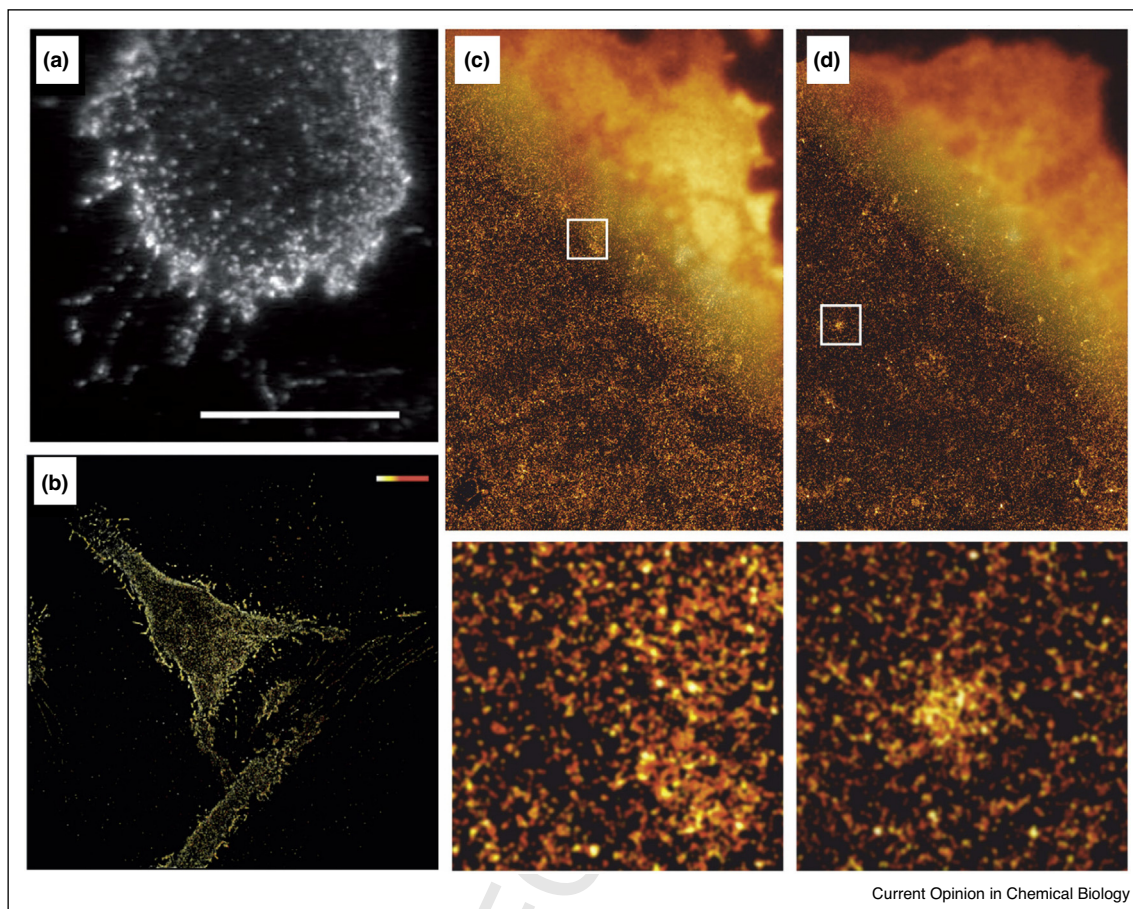
206 On a larger spatial scale, chemoenzymatic labeling pro-  
207 tocols have demonstrated that it is possible to obtain  
208 images of tissue with glycan labeling that augments  
209 histological hematoxylin and eosin staining. In order to  
210 emphasize the capabilities of the approach, Rouhanifard,  
211 Lopez-Aguilar and Wu refer to this as: ‘chemoenzymatic  
212 labeling histology method using clickable probes’  
213 (CHoMP) [35\*\*]. **Figure 3a** and **b** shows the results of  
214 this chemoenzymatic approach with LacNAc labeling of  
215 lung tissue obtained from a fixed/frozen 10  $\mu\text{m}$  mouse  
216 tissue section [35\*\*]. This group also applied this method  
217 to other tumor tissue and to screening human tumor  
218 microarrays, where it was observed that there was a  
219 large, 13-fold decrease in LacNAc expression in grade  
220 1 lung adenocarcinoma patient samples as compared with  
221 healthy humans.  
222

223 Bioorthogonal labeling of several organ systems in living  
224 animals (e.g. heart, liver and kidney) has recently been  
225 expanded to include sialylated glycans in the brain of live  
226 mice using intravenous injection of PEGylated liposomes  
227 encapsulating 9AzSia or ManNAz that were able to cross  
228 the blood brain barrier [36\*\*]. Because this liposome-  
229 assisted bioorthogonal reporter (LABOR) strategy can  
230 also be combined with histological staining, it is possible  
231 to relate the spatial distribution of sialylated glycans to  
232 features such as synaptic density.  
233

234 **Figure 3c** and **d** shows labeling that was achieved with  
235 LABOR strategy using 9AzSia coupled with *in vivo* cop-  
236 per-free click chemistry. These confocal images delineate  
237 the distribution of 9AzSia-incorporated sialoglycans in the  
238 granule cell layer of dentate gyrus in the hippocampus.  
239 Using 10  $\mu\text{m}$  thick sections with glycan labeling and co-  
240 immunostaining using synaptophysin and DAPI, multi-  
241 colored images highlight the biosynthesis and distribu-  
242 tion of sialic acids on cell surfaces and synapses (as labeled

## 4 Molecular imaging

Figure 2



Single molecule tracking and STORM imaging. **(a)** Snapshot of Alexa Fluor 647 molecules on N-linked sialic acid in a live metastatic cell using TIRFM. Scale bar = 20  $\mu\text{m}$ . Adapted from Jiang *et al.* [30]. **(b)** STORM imaging of sialic acid on live HeLa cells, metabolically labeled with  $\text{Ac}_4\text{ManNAI}$  and conjugated with Alexa Fluor 647 azide using BTTPS/ $\text{Cu}'$  catalyst. The image was produced from 480 consecutive frames with 130021 detected deviation equal to the localization precision. The color bar represents the integrated fluorescent intensity of each molecule. Scale bar = 10  $\mu\text{m}$ . Adapted from Jiang *et al.* [30]. **(c)** STORM image obtained from fixed human osteosarcoma (U2OS) cells metabolically labeled with  $\text{Ac}_4\text{GalNAz}$  and clicked with CuAAC. Adapted from Mateos-Gil *et al.* [34]. **(d)** STORM image obtained from U2OS cells metabolically labeled with  $\text{Ac}_4\text{GalNAz}$  using copper-free strain-promoted azide-alkyne cycloaddition. Adapted from Mateos-Gil *et al.* [34] (boxed region = 2.0  $\mu\text{m}$  wide).

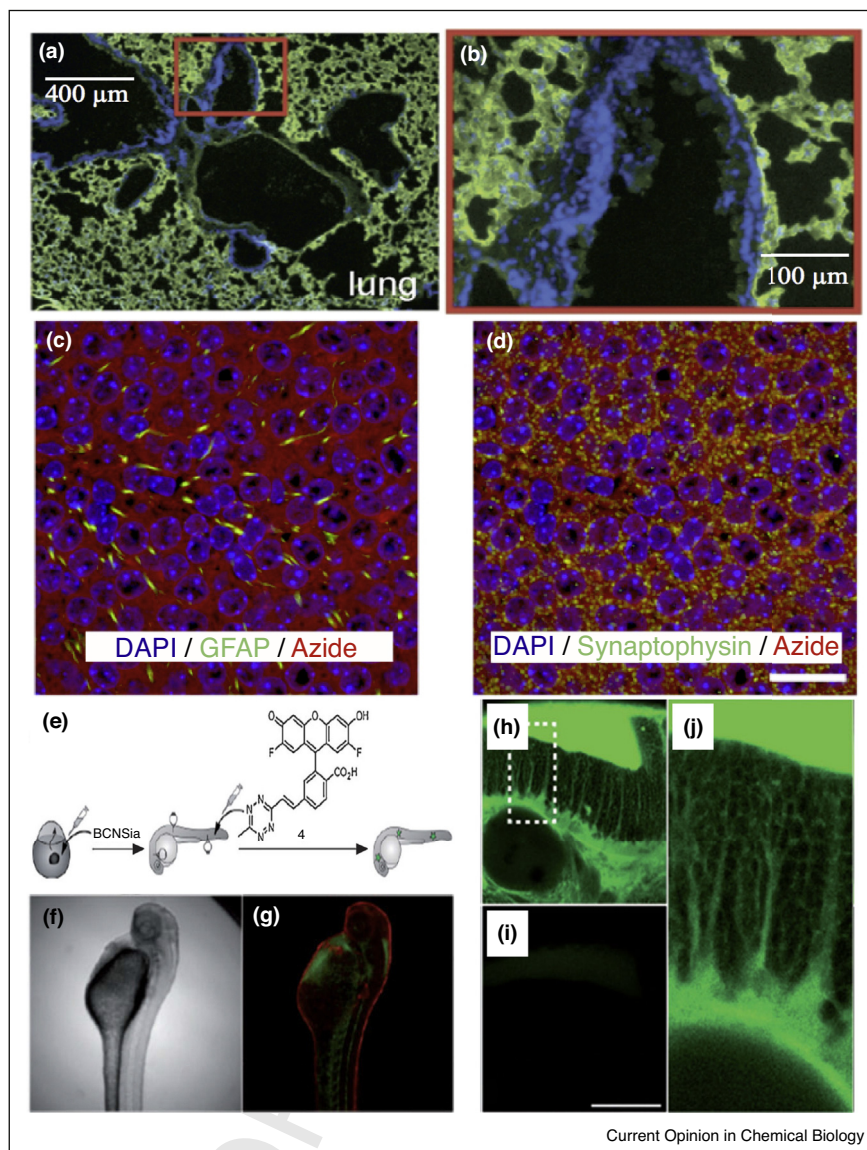
with synaptophysin) and a marker for astrocytes glial fibrillary acidic protein (GFAP).

Since the chemical reporter strategy was first applied to image surface glycans in developing zebrafish a decade ago [38], this model organism has remained the subject for advances in bioorthogonal chemistry which seek to overcome the limitations of imaging internal structures with exogenous probes. In order to prevent the high background fluorescence from unreacted probe, which can dominate glycan imaging in the transparent zebrafish, Bertozzi's group developed an alternative approach exploiting the direct injection of a cyclooctyne-functionalized sialic acid followed by subsequent injection of a turn-on tetrazine probe [37\*]; using this approach, they

were able to demonstrate new sialylated structures in the developing zebrafish.

Although not as efficiently incorporated as  $\text{Ac}_4\text{ManNAz}$ , microinjection of a bicyclononyne-functionalized sialic acid derivative, BCNSia, followed by injection of a fluorogenic cyclooctyne-reactive probe enabled imaging of zebrafish embryogenesis, with minimal background fluorescence. Agarwal *et al.* demonstrated that prior to the copper click chemistry reaction, the new probe produced minimal background fluorescence, but robust SiaNAI-dependent labeling of enveloping layer cells following reaction [37\*]. Figure 3e shows their approach to labeling with BCNSia and 4 and images from (f and g) embryos injected with BCNSia (and fluorogenic probe CalFluor

Figure 3



Tissue and whole animal imaging. **(a and b)** Chemoenzymatic labeling using clickable probes (CHoMP) applied to LacNAc labeling of lung tissue obtained from a fixed/frozen 10  $\mu\text{m}$  mouse tissue section (Green: LacNAc staining; Blue: DAPI nuclear staining) Adapted from Rouhanifard *et al.* [35\*\*]. **(c and d)** Liposome-assisted bioorthogonal reporter (LABOR) strategy used to label sialylated glycans in the dentate gyrus in mouse hippocampus with an azido sialic acid reporter molecule and copper-free click chemistry. Confocal images obtained from 10  $\mu\text{m}$  thick sections with immunostaining using synaptophysin, DAPI and the marker for astrocytes, glial fibrillary acidic protein (GFAP). Adapted from Xie *et al.* [36\*\*]. **(e)** Schema for sialylation imaging in live Zebrafish embryos with BCNSia and injection with **4**. Adapted from Agarwal *et al.* [37\*]. **(f and g)** Brightfield and embryo injected with BCNSia at the 1–8 cell stage and injected with **4** and bathed in a copper click solution with CalFluor 647. Adapted from Agarwal *et al.* [37\*]. **(h–j)** Zebrafish lateral view of hindbrain, (i) injections with vehicle. Scale bar = 100  $\mu\text{m}$ . Adapted from Agarwal *et al.* [37\*].

647 to map the vasculature). **Figure 3h** and **j** shows lateral views of labeled hindbrain and absence of labeling with injection of vehicle, **Figure 3i**.

### Perspectives and conclusions

The applications presented in this review demonstrate that the leading microscopic methods, which have

revolutionized the study of proteins in living systems, can be adapted to imaging glycans on single cells and tissues. Bioorthogonal chemical reporter strategies, using metabolic oligosaccharide engineering and CeGL, have enabled the application of FRAP, single molecule tracking and super-resolution imaging. This strategy, when combined with genetically encoded probes, has made it

## 6 Molecular imaging

possible to visualize glycans on a specific protein via FRET and FLIM. Furthermore, it has now been demonstrated that neither the blood brain barrier nor the enveloping layer prevents *in vivo* imaging of sialylated glycans. In the not too distant future, there will be many examples of application of these new techniques to characterize glycosylation changes associated with animal models of human disease and on human samples.

## Acknowledgements

B.O. and P.W. acknowledge support from NIH (GM111938) and P.W. acknowledges support from NIH (GM093282 and GM113046).

## References and recommended reading

Papers of particular interest, published within the period of review, have been highlighted as:

- of special interest
- of outstanding interest

1. Chuh KN, Batt AR, Pratt MR: **Chemical methods for encoding and decoding of posttranslational modifications.** *Cell Chem Biol* 2016, **23**:86-107.
  2. Hang HC, Yu C, Kato DL, Bertozzi CR: **A metabolic labeling approach toward proteomic analysis of mucin-type o-linked glycosylation.** *Proc Natl Acad Sci U S A* 2003, **100**:14846-14851.
  3. Sletten EM, Bertozzi CR: **Bioorthogonal chemistry: fishing for selectivity in a sea of functionality.** *Angew Chem Int Ed Engl* 2009, **48**:6974-6998.
  4. Saxon E, Bertozzi CR: **Cell surface engineering by a modified staudinger reaction.** *Science*. 2000, **287**:2007-2010.
  5. Saxon E, Luchansky SJ, Hang HC, Yu C, Lee SC, Bertozzi CR: **Investigating cellular metabolism of synthetic azidosugars with the staudinger ligation.** *J Am Chem Soc* 2002, **124**:14893-14902.
  6. McKay CS, Finn MG: **Click chemistry in complex mixtures: bioorthogonal bioconjugation.** *Chem Biol* 2014, **21**:1075-1101.
  7. Baskin JM, Prescher JA, Laughlin ST, Agard NJ, Chang PV, Miller IA, Lo A, Codelli JA, Bertozzi CR: **Copper-free click chemistry for dynamic in vivo imaging.** *PNAS* 2007, **104**:16793-16797.
  8. Chang PV, Prescher JA, Sletten EM, Baskin JM, Miller IA, Agard NJ, Lo A, Bertozzi CR: **Copper-free click chemistry in living animals.** *PNAS* 2010, **107**:1821-1826.
- This is the first example of applying Copper-free click chemistry to visualize the dynamic trafficking of glycans in live cells.
9. Soriano D, Wang W, Jiang H, Besanceney C, Yan AC, Levy M, Liu Y, Marlow FL, Wu P: **Biocompatible copper (I) catalysts for in vivo imaging of glycans.** *J Am Chem Soc* 2010, **132**:16893-16899.
  10. Wang W, Hong S, Tran A, Jiang H, Triano R, Liu Y, Chen X, Wu P: **Sulfated ligands for the copper(I)-catalyzed azide-alkyne cycloaddition.** *Chem Asian J* 2011, **6**:2796-2802.
  11. Besanceney-Webler C, Jiang H, Zheng T, Feng L, Soriano del Amo D, Wang W, Klivansky LM, Marlow FL, Liu Y, Wu P: **Increasing the efficacy of bioorthogonal click reactions for bioconjugation: a comparative study.** *Angew Chem Int Ed* 2011, **50**:8051-8056.
- New biocompatible ligands assisted copper-catalyzed azide-alkyne cycloaddition has demonstrated unsurpassed bioconjugation efficiency.
12. Dube D, Bertozzi C: **Glycans in cancer and inflammation-potential for therapeutics and diagnostics.** *Nat Rev Drug Discov* 2005, **4**:477.
  13. Lopez Aguilar A, Briard JG, Yang L, Ovrzyn B, Macauley MS, Wu P: **Tools for studying glycans: recent advances in chemoenzymatic glycan labeling.** *ACS Chem Biol* 2017, **12**:611-621.
- Describes development and recent applications of chemoenzymatic glycan labeling.
14. Laughlin ST, Bertozzi CR: **Imaging the glycome.** *PNAS* 2009, **106**:12-17.
  15. Bertozzi CR: **A decade of bioorthogonal chemistry.** *Acc Chem Res* 2011, **44**:651-653.
  16. Doll F, Buntz A, Spate A-K, Scharf VF, Timper A, Schrimpf W, Hauck CR, Zumbusch A, Wittmann V: **Visualization of protein-specific glycosylation inside living cells.** *Angew Chem Int Ed Engl* 2016, **55**:2262-2266.
  17. Lin L, Tian X, Hong S, Dai P, You Q, Wang R, Feng L, Xie C, Tian Z-Q, Chen X: **A bioorthogonal Raman reporter strategy for sers detection of glycans on live cells.** *Angew Chem Int Ed Engl* 2013 Jul, **52**:7266-7271.
- Provides demonstration of surface enhanced Raman scattering from label glycans in live cells.
18. Neves AA, Wainman YA, Wright A, Kettunen MI, Rodrigues TB, McGuire S, Hu D-E, Bulat F, Geninatti Crich S, Stockmann H, Leeper FJ, Brindle KM: **Imaging glycosylation in vivo by metabolic labeling and magnetic resonance imaging.** *Angew Chem Int Ed Engl* 2016, **55**:1286-1290.
  19. Chuh KN, Pratt MR: **Chemistry-enabled methods for the visualization of cell-surface glycoproteins in metazoans.** *Glycoconj J* 2015, **32**:443-454.
  20. Zheng M, Zheng L, Zhang P, Li J, Zhang Y: **Development of bioorthogonal reactions and their applications in bioconjugation.** *Molecules* 2015, **20**:3190-3205.
  21. Li S, Wang L, Yu F, Zhu Z, Shobaki D, Chen H, Wang M, Wang J, Qin G, Erasquin UJ, Ren L, Wang Y, Cai C: **Copper-catalyzed click reaction on/in live cells.** *Chem Sci* 2017, **8**:2107-2114.
  22. Jiang H, Zheng T, Lopez-Aguilar A, Feng L, Kopp F, Marlow FL, Wu P: **Monitoring dynamic glycosylation in vivo using supersensitive click chemistry.** *Bioconjug Chem* 2014, **25**:698-706.
- This paper demonstrated that the introduction of an electron-donating picolyl azide combined with BTTPS-a tris(triazolylmethyl)amine based ligand for Cu(I)-produced at least a 20-fold enhancement of CuAAC fluorescent labeling.
23. Wier M, Edidin M: **Constraint of the translational diffusion of a membrane glycoprotein by its external domains.** *Science* 1988, **242**:412.
  24. Edidin M: **Class I MHC molecules as probes of membrane patchiness: from biophysical measurements to modulation of immune responses.** *Immunol Res* 2010, **47**:265.
  25. Edidin M, Zú niga MC, Sheetz MP: **Truncation mutants define and locate cytoplasmic barriers to lateral mobility of membrane glycoproteins.** *Proc Natl Acad Sci U S A* 1994, **91**:3378-3382.
  26. Rodriguez-Rivera FP, Zhou X, Theriot JA, Bertozzi CR: **Visualization of mycobacterial membrane dynamics in live cells.** *J Am Chem Soc* 2017, **139**:3488-3495.
  27. Lin W, Du Y, Zhu Y, Chen X: **A cis-membrane fret-based method for protein-specific imaging of cell-surface glycans.** *J Am Chem Soc* 2014, **136**:679-687.
  28. Fernandez-Suarez M, Baruah H, Martinez-Hernandez L, Xie KT, Baskin JM, Bertozzi CR, Ting AY: **Redirecting lipoic acid ligase for cell surface protein labeling with small-molecule probes.** *Nat Biotechnol* 2007, **25**:1483-1487.
  29. Belardi B, De La Zerda A, Spiciarich DR, Maund SL, Peehl DM, Bertozzi CR: **Imaging the glycosylation state of cell surface glycoproteins by two-photon fluorescence lifetime imaging microscopy.** *Angew Chem Int Ed* 2013, **52**:14045-14049.
  30. Jiang H, Wu P, Ovrzyn B: **Super-resolution imaging and single-molecule tracking of glycans on the surface of live cells.** In *Focus on Microscopy*. Edited by Brakenhoff F. 2013:503.
  31. Jiang H, English BP, Hazan RB, Wu P, Ovrzyn B: **Tracking surface glycans on live cancer cells with single-molecule sensitivity.** *Angew Chem Int Ed Engl* 2015, **54**:1765-1769.

- 419 This was the first demonstration of super-resolution imaging of glycans  
420 in live cells. Single molecule tracking of metabolically labeled glycans  
421 was also implemented. The authors used a ligand assisted copper  
422 catalyst. 435
- 423 32. Letschert S, Göhler A, Franke C, Bertleff-Zieschang N, Memmel E,  
424 •• Doose S, Seibel J, Sauer M: **Super-resolution imaging of plasma**  
425 **membrane glycans**. *Angew Chem* 2014, **126**:11101-11104. 436
- 426 Using copper-free click chemistry the authors implemented dSTORM in  
427 fixed cells. 437
- 428 33. Atilgan E, Ovrzyn B: **Nucleation and growth of integrin**  
429 **adhesions**. *Biophys J* 2009, **96**:3555-3572. 438
- 430 34. Mateos-Gil P, Letschert S, Doose S, Sauer M: **Super-resolution**  
431 **imaging of plasma membrane proteins with click chemistry**.  
432 *Front Cell Dev Biol* 2016, **4**:98. 439
- 433 35. Rouhanifard SH, Lopez-Aguilar A, Wu P: **CHoMP: A**  
434 **chemoenzymatic histology method using clickable probes**.  
435 *Chembiochem* 2014, **15**:2667-2673. 440
- This article presents the first example of using bioorthogonal chemical  
reporter strategy to analyze glycosylation patterns in human tissue  
samples. 441
36. Xie R, Dong L, Du Y, Zhu Y, Hua R, Zhang C, Chen X: **In vivo**  
•• **metabolic labeling of sialoglycans in the mouse brain by using**  
• **a liposome-assisted bioorthogonal reporter strategy**. *Proc Natl*  
*Acad Sci U S A* 2016, **113**:5173-5178. 442
- Demonstration that the blood brain barrier does not prevent bioortho-  
gonal labeling of sialylated glycans in live animals 443
37. Agarwal P, Beahm BJ, Shieh P, Bertozzi CR: **Systemic**  
• **fluorescence imaging of zebrafish glycans with bioorthogonal**  
**chemistry**. *Angew Chem Int Ed Engl* 2015, **54**:11504-11510. 444
- Circumvents the use of exogenous probes for labeling sialylated glycans  
in zebrafish embryogenesis 445
38. Laughlin ST, Baskin JM, Amacher SL, Bertozzi CR: **In vivo**  
**imaging of membrane-associated glycans in developing**  
**zebrafish**. *Science* 2008, **320**:664-667. 446
- 447 448 449 450 451 452